

WHAT TYPES OF JETS DOES NATURE MAKE: A NEW POPULATION OF RADIO QUASARS

PAOLO PADOVANI¹, ERIC S. PERLMAN², HERMINE LANDT³

Space Telescope Science Institute, 3700 San Martin Drive, Baltimore, MD 21218, USA

AND

PAOLO GIOMMI, MATTEO PERRI⁴

ASI Science Data Center, ASDC, c/o ESRIN, Via G. Galilei, I-00044 Frascati, Italy

Draft version October 30, 2018

ABSTRACT

We use statistical results from a large sample of about 500 blazars, based on two surveys, the Deep X-ray Radio Blazar Survey (DXRBS), nearly complete, and the RASS-Green Bank survey (RGB), to provide new constraints on the spectral energy distribution of blazars, particularly flat-spectrum radio quasars (FSRQ). This reassessment is prompted by the discovery of a population of FSRQ with spectral energy distribution similar to that of high-energy peaked BL Lacs. The fraction of these sources is sample dependent, being $\sim 10\%$ in DXRBS and $\sim 30\%$ in RGB (and reaching $\sim 80\%$ for the *Einstein* Medium Sensitivity Survey). We show that these “X-ray strong” radio quasars, which had gone undetected or unnoticed in previous surveys, indeed are the strong-lined counterparts of high-energy peaked BL Lacs and have synchrotron peak frequencies, ν_{peak} , much higher than “classical” FSRQ, typically in the UV band for DXRBS. Some of these objects may be 100 GeV – TeV emitters, as are several known BL Lacs with similar broadband spectra. Our large, deep, and homogeneous DXRBS sample does not show anti-correlations between ν_{peak} and radio, broad line region, or jet power, as expected in the so-called “blazar sequence” scenario. However, the fact that FSRQ do not reach X-ray-to-radio flux ratios and ν_{peak} values as extreme as BL Lacs and the elusiveness of high ν_{peak} –high-power blazars suggest that there might be an intrinsic, physical limit to the synchrotron peak frequency that can be reached by strong-lined, powerful blazars. Our findings have important implications for the study of jet formation and physics and its relationship to other properties of active galactic nuclei.

Subject headings: galaxies: active — BL Lacertae objects: general — quasars: general — radiation mechanisms: non-thermal — radio continuum: galaxies — X-rays: galaxies

1. A PHENOMENOLOGICAL DESCRIPTION OF THE BLAZAR CLASS

Blazars are one of the most extreme classes of active galactic nuclei (AGN), distinguished by high luminosity, rapid variability, high polarization, radio core-dominance, and apparent superluminal speeds (Urry & Padovani 1995). Their broad-band emission extends from the radio up to the gamma-ray band, and is dominated by non-thermal processes. The blazar class includes BL Lacertae objects, characterized by an almost complete lack of emission lines, and the flat-spectrum radio quasars (FSRQ), which by definition display broad, strong emission lines.

More than 95% of all known blazars have been discovered either in radio or X-ray surveys (Padovani & Giommi 1995a). Previous work has shown that X-ray and radio selection methods yield objects with somewhat different properties at least for BL Lacs. The energy output of most radio selected BL Lacs peaks in the IR/optical (Giommi & Padovani 1994; Padovani & Giommi 1995b, 1996). These objects are more highly polarized (Jannuzi, Smith, & Elston 1994), and are more core-dominated in the radio (Perlman & Stocke 1993; Laurent-Muehleisen et

al. 1993; Kollgaard et al. 1996; Rector, Stocke, & Perlman 1999) and are now referred to as LBL (low-energy peaked BL Lacs). By contrast, the energy output of most X-ray selected BL Lacs peaks in the UV/X-ray; these objects, which are referred to as HBL (high-energy peaked BL Lacs), are less polarized and generally have preferred position angles of polarization in the optical (Jannuzi, Smith, & Elston 1994), and are less core-dominant in the radio (Perlman & Stocke 1993; Kollgaard et al. 1996; Rector et al. 2000).

Padovani & Giommi (1995b) have demonstrated that the difference in broad-band peaks for HBL and LBL is not simply phenomenological. Rather, it represents a fundamental difference between the two sub-classes. In this respect, one could expect to find a similar division in the FSRQ class – for which, until recently, no evidence existed. Indeed, it was suggested by some authors (Samburina, Maraschi & Urry 1996), based upon the similarities of the optical–X-ray broad-band spectral characteristics of LBL and FSRQ, that no FSRQ with synchrotron peak emission in the UV/X-ray band should exist.

The dichotomy that there existed both high and low energy peaked BL Lacs (but virtually no intermediate ob-

¹ ESA Space Telescope Division² Joint Center for Astrophysics, University of Maryland, 1000 Hilltop Circle, Baltimore, MD 21250, USA (current address)³ Hamburger Sternwarte, Gojenbergsweg 112, D-21029 Hamburg, Germany⁴ Dipartimento di Fisica, Università la Sapienza, P.le A. Moro 2, Roma, Italy

jects), and only low energy peaked FSRQ was the state of the art in our knowledge of blazar spectral energy distributions (SEDs) in the mid 1990s. Four discoveries have drastically changed this picture:

1. The multi-frequency catalog of Padovani, Giommi, & Fiore (1997), which included all FSRQ known before DXRBS and other recent surveys, identified more than 50 FSRQ ($\sim 17\%$ of the FSRQ in their catalog) with broad-band spectra similar to those of HBL.
2. About 30% of FSRQ found in the Deep X-ray Radio Blazar Survey (DXRBS; Perlman et al. 1998; Landt et al. 2001) were found to have X-ray-to-radio luminosity ratios, L_x/L_r , typical of HBL ($L_x/L_r \gtrsim 10^{-6}$ or $\alpha_{rx} \lesssim 0.78$), but broad (full width half maximum $> 2,000 \text{ km s}^{-1}$) and luminous ($L > 10^{43} \text{ erg s}^{-1}$) emission lines typical of FSRQ.
3. The discovery of large numbers of “intermediate” BL Lacs, objects with broadband properties intermediate between HBL and LBL, in the DXRBS (Perlman et al. 1998; Landt et al. 2001), ROSAT-Green Bank (RGB; Laurent-Muehleisen et al. 1998) and other samples (Nass et al. 1996; Kock et al. 1996).
4. *BeppoSAX* observations have shown that the X-ray emission of at least one FSRQ is dominated by synchrotron radiation, with a peak frequency $\nu_{\text{peak}} \sim 2 \times 10^{16} \text{ Hz}$ and steep ($\alpha_x \sim 1.5$) X-ray spectrum (Padovani et al. 2002). Two more FSRQ show evidence of $\nu_{\text{peak}} \approx 10^{15} \text{ Hz}$.

The discovery of “X-ray strong” FSRQ (labeled HFSRQ by Perlman et al. 1998 to parallel the HBL moniker; the “standard” FSRQ would then be the LFSRQ) represents a fundamental change in our perception of the broadband spectrum of FSRQ, similar to that brought about by the X-ray selected BL Lacs discovered in the *Einstein* Medium Sensitivity Survey (EMSS) (Morris et al. 1991; Stocke et al. 1991; Rector et al. 2000). A preliminary investigation of the properties of HFSRQ in the DXRBS survey was presented in Perlman et al. (1998). The discovery of a large number of intermediate BL Lacs should have been in many ways expected already in the mid 1990s given our knowledge of the vastly disparate parameter space coverages of X-ray and radio surveys (see § 3).

With these recent discoveries in mind, it is time to once again take stock of the broadband spectral properties of all blazars. Here we utilize updated identifications from DXRBS (most of which were presented by Landt et al. 2001), which result in a much larger sample, combined with a sample of blazars we have extracted from RGB (Laurent-Muehleisen 1996; Laurent-Muehleisen et al. 1998), to attack this problem. A preliminary version of some of these findings was presented previously by Perlman (2000).

The samples are briefly described in § 2. In § 3 we comment on the failure of previous surveys to find X-ray strong FSRQ. In § 4 we study the SEDs of our sources and discuss the use of the available data to obtain the peak frequency of synchrotron emission and other characteristics

of blazars. We discuss the so-called “blazar sequence” scenario in § 5 and further constraints on blazar emission in § 6, while § 7 summarizes our conclusions. Throughout this paper spectral indices are written $S_\nu \propto \nu^{-\alpha}$ and for consistency with previous work the values $H_0 = 50 \text{ km s}^{-1} \text{ Mpc}^{-1}$, $\Omega_M = 0$, and $\Omega_\Lambda = 0$ have been adopted. We note that our correlations (or lack of) are basically unchanged for a cosmological model with $H_0 = 65 \text{ km s}^{-1} \text{ Mpc}^{-1}$, $\Omega_M = 0.3$, and $\Omega_\Lambda = 0.7$.

2. THE SAMPLES

2.1. The DXRBS Blazar Sample

DXRBS is the result of correlating the ROSAT WGA-CAT database (White, Giommi, & Angelini 1995) with several publicly available radio catalogs (GB6 and PMN at 5 GHz, NORTH20CM at 1.4 GHz), restricting the candidate list to serendipitous flat-spectrum radio sources ($\alpha_r \leq 0.70$). Additionally, a snapshot survey with the Australia Telescope Compact Array (ATCA) was conducted for $\delta \lesssim 0^\circ$ to get radio spectral indices unaffected by variability (and arc-second positions for the sources south of $\delta = -40^\circ$, the limit of the NRAO-VLA Sky Survey [NVSS]; Condon et al. 1998). The DXRBS X-ray flux limits depend on the exposure time and the distance from the center of the ROSAT Position Sensitive Proportional Counter (PSPC) but vary between $\sim 10^{-14}$ and $\sim 10^{-11} \text{ erg cm}^{-2} \text{ s}^{-1}$. Radio 5 GHz fluxes reach down to $\sim 50 \text{ mJy}$.

First results from DXRBS were presented in Perlman et al. (1998), while updated identifications were presented in Landt et al. (2001). At the time of writing (November 2002), DXRBS includes 244 blazars: 200 FSRQ (defined as broad-line sources with $\alpha_r \leq 0.50$) and 44 BL Lacs. Details on our BL Lac classification are given in Landt et al. (2001). Note that Giommi et al. (2002b) have pointed out that sources with optical spectrum typical of a galaxy but nuclear SED typical of a blazar should probably be classified as low-luminosity BL Lacs. Some of our radio galaxies might fall in that category. We will address this point in future papers.

We include in this work only sources belonging to the complete sample, which fulfills all our selection criteria (see details in Landt et al. 2001). This is necessary because we want to compare in detail the properties (mainly the SED) of DXRBS FSRQ and BL Lacs and that requires well-defined samples, not to introduce any bias. Since we need the sky coverage to de-convolve the observed distributions, we have excluded sources with PSPC center offsets in the range $13' - 24'$, where the sky coverage is difficult to determine because of the effects of the spacecraft wobble and the rib structure. We are then left with 134 FSRQ and 31 BL Lacs, for a total of 165 blazars. Only about 10 more sources ($\sim 5\%$ of the total) with $\alpha_r \leq 0.50$ remain to be identified. The current blazar sample is therefore highly representative.

2.2. The RGB Blazar Sample

Laurent-Muehleisen et al. (1997) have described in depth the procedures undertaken in constructing the ROSAT All Sky Survey (RASS)-Green Bank (RGB) catalog of radio and X-ray emitting sources. Here we review only the essential points.

The catalog was constructed by correlating the RASS with a radio catalog based on the 1987 Green Bank 5 GHz survey maps (Gregory & Condon 1991; Gregory et al. 1996). VLA observations of all the 2,127 radio/X-ray matches within $100''$ were obtained to derive arc-second positions (Laurent-Muehleisen et al. 1997). For the 1,567 sources with radio/X-ray offset $< 40''$ optical counterparts were identified using the Automatic Plate Measuring (APM) scans (Irwin, Maddox, & McMahon 1994), which give O (blue) and E (red) magnitudes. Laurent-Muehleisen et al. (1997, 1998) give many new object identifications based upon spectra taken at various optical telescopes. The identifications published by Laurent-Muehleisen et al. (1997, 1998) include a comprehensive list of BL Lacs, as well as many radio-loud, broad-line objects (i.e., radio-loud quasars); however, since radio spectral index was not included in the search criteria for RGB no list of FSRQ was compiled there.

Some indication that X-ray strong FSRQ were being found in the RGB sample could be seen from the distribution of X-ray to radio flux ratios of the newly identified objects (Laurent-Muehleisen et al. 1998). We therefore decided to use the information in the RGB along with other public surveys to create a list of all blazars (BL Lacs and FSRQ) in the full RGB sample. We used Tables 3.3 and 3.4 of Laurent-Muehleisen (1996) and Table 3 of Laurent-Muehleisen et al. (1998) to search for both BL Lacs and FSRQ as follows. First, the RGB sample was cross-correlated with the AGN catalog of Padovani, Giommi, & Fiore (1997) to find previously known blazars. Then, we used the identifications given by Laurent-Muehleisen et al. (1998) to include newly identified sources (note that these are limited to objects with $O \leq 18.5$). This resulted in a total of more than 600 classified RGB sources. Being based on the RASS, the RGB covers a very different X-ray flux range: X-ray fluxes range between $\sim 2 \times 10^{-13}$ and $\sim 10^{-10}$ erg cm $^{-2}$ s $^{-1}$. Radio 5 GHz fluxes reach down to ~ 25 mJy, roughly a factor of 2 fainter than DXRBS at similar declinations.

Radio spectral indices, necessary to determine if a broad-line radio source is an FSRQ or not, were derived by cross-correlating the RGB with the NVSS. For consistency with DXRBS, we used 5 GHz fluxes from the GB6 survey (and not from the dedicated VLA observations) for the RGB sources. In doing the cross-correlation, then, the 1.4 GHz flux from all NVSS sources within a $3'$ radius (corresponding roughly to the beam size of the GB6 survey) was summed up (we have already described the rationale connected with doing this in Perlman et al. 1998). We then isolated a sample of FSRQ ($\alpha_r \leq 0.5$).

We checked that the spectral indices derived from the GB6/NVSS radio data were reliable in the following way. Three hundred and forty-five radio-loud RGB sources had a value of the radio spectral index in the AGN catalog of Padovani, Giommi, & Fiore (1997), generally obtained from non-simultaneous, single-dish measurements around a few GHz. There is a very strong ($P > 99.99\%$) linear correlation with a slope ~ 0.9 between the two spectral indices, with a mean difference $\Delta\alpha = 0.08$ over a range of ~ 2.5 . This shows that the method we used to estimate the radio spectral index for the RGB sample is quite robust.

The RGB blazar sample thus includes 362 blazars: 233 FSRQ and 129 BL Lacs. To our knowledge the RGB sample is $\sim 44\%$ identified. This fraction goes up to $\sim 76\%$ for the part of the sample with $O \leq 18.5$. Considering only the sources with $\alpha_r \leq 0.5$, these fractions do not change much, being 49% and 73% respectively.

2.3. The Joint Sample

Overall, the two samples used in this paper include 497 distinct blazars, 342 FSRQ and 155 BL Lacs (30 objects are in common). In terms of its range of properties, size, depth, and selection criteria this ensemble of objects represents a unique sample with which to address some of the open questions of blazar research.

As an initial step towards studying the broad-band properties of our sources, we first derive their α_{ox} , α_{ro} , and α_{rx} values. These are the usual rest-frame effective spectral indices defined between 5 GHz, 5,000 Å, and 1 keV. X-ray and optical fluxes have been corrected for Galactic absorption. The effective spectral indices have been k-corrected using the appropriate radio, optical, and X-ray spectral indices. X-ray spectral indices are available for all DXRBS sources from hardness ratios, as described in Landt et al. (2001). For the RGB objects we obtained X-ray spectral indices from hardness ratios for 73% and 89% of FSRQ and BL Lacs respectively from Brinkmann et al. (1997), Laurent-Muehleisen et al. (1999), Reich et al. (2000), and WGACAT. In the remaining cases we assumed $\alpha_x = 1.2$ following Laurent-Muehleisen et al. (1998). Values for the optical spectral indices were assumed to be the typical ones for the various sub-classes. Finally, optical magnitudes for broad-line sources were also corrected for the presence of emission lines according to the prescription of Natali et al. (1998).

It is worth mentioning that, unlike DXRBS, all new RGB identifications have $O \leq 18.5$. This has important selection biases associated with it (§§ 3,4). In particular, an optical magnitude limit has the effect of imposing an artificial boundary on the regions of parameter space to which a survey is sensitive. Namely, only sources with $\alpha_{\text{ro}} < \alpha_{\text{ro}}(\text{lim})$ and $\alpha_{\text{ox}} > \alpha_{\text{ox}}(\text{lim})$, where these limiting values depend on radio and X-ray flux, will be included. At the survey radio limit, for example, only sources with $\alpha_{\text{ro}} \lesssim 0.4$ will be included. We will discuss the effect of this limitation in § 4.

3. THE DISCOVERY OF X-RAY STRONG FSRQ

The findings of Padovani, Giommi, & Fiore (1997), Perlman et al. (1998), and Padovani et al. (2002), make it clear that detecting X-ray strong FSRQ requires large and/or deep samples. It was already known in 1995 that radio-selected samples find more frequently objects with broad-band spectra peaking in the IR/optical. The oft-repeated separation of HBL and LBL on the $\alpha_{\text{ox}}, \alpha_{\text{ro}}$ plane (e.g., Padovani & Giommi 1995b), is a direct by-product of these disjoint survey methods.

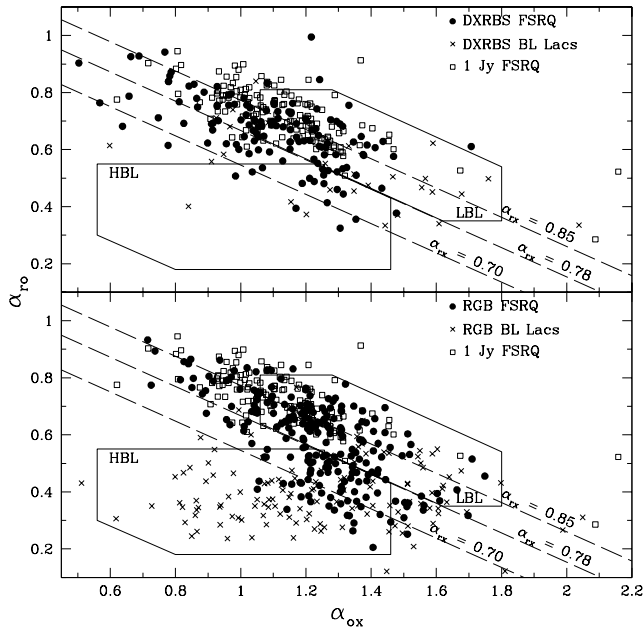


FIG. 1.— The α_{ro} , α_{ox} plane for the DXRBS (top) and RGB (bottom) samples. Effective spectral indices are defined in the usual way and calculated between the rest-frame frequencies of 5 GHz, 5000 Å, and 1 keV. Filled circles represent the DXRBS and RGB FSRQ, open squares represent the 1 Jy FSRQ, while crosses are the DXRBS and RGB BL Lacs. The dashed lines represent, from top to bottom, the loci of $\alpha_{\text{rx}} = 0.85$, typical of 1 Jy FSRQ and LBL, $\alpha_{\text{rx}} = 0.78$, the dividing line between HBL and LBL, and $\alpha_{\text{rx}} = 0.70$, typical of RGB BL Lacs. The regions in the plane within 2σ from the mean α_{ro} , α_{ox} , and α_{rx} values of LBL and HBL are indicated by the solid lines and marked accordingly.

With this observation in mind, one might expect a similar selection effect to have been present for FSRQ. Yet up until the mid-1990s, no X-ray survey had looked for FSRQ, even though re-examinations of the *Einstein* EMSS and Slew Survey databases have revealed samples of FSRQ in both (Perlman 2000; Perlman et al. 2001; Wolter & Celotti 2001). The only flux-limited samples of FSRQ which existed prior to that time, in fact, were “classical” high flux limit, radio-selected samples, such as the 1 Jy, produced by surveys which also contained few, if any HBL (e.g., the 1 Jy sample has only 2 HBL out of 34 BL Lacs total, Padovani & Giommi 1995b). Thus it was perhaps not a surprise that these radio-selected samples contained very few X-ray strong FSRQ.

Figure 1 shows the distribution of our sources in the α_{ox} , α_{ro} plane. The figure shows also the 1 Jy FSRQ, which occupy a region of α_{ox} , α_{ro} parameter space with α_{rx} similar to that typical of LBL (marked in the figure). FSRQ with low α_{rx} ($\lesssim 0.78$, roughly equivalent to the HBL/LBL division (although see § 4), or $L_{\text{x}}/L_{\text{r}} \gtrsim 10^{-6}$) constitute only $\sim 5\%$ of the 1 Jy sources with X-ray data. Importantly, none of the 1 Jy FSRQ fall in the region of the plane within 2σ from the mean α_{ro} , α_{ox} , and α_{rx} values of HBL, the “HBL box”, derived by using all HBL in the multi-frequency AGN catalog of Padovani, Giommi, & Fiore (1997)⁵. The fainter radio/X-ray selected DXRBS and RGB FSRQ, on the other hand, reach much lower

values of α_{rx} and many sources “invade” the HBL region. Indeed, as can be seen by comparing the two panels of Figure 1, there is a progression of α_{ox} , α_{ro} from 1 Jy to DXRBS to RGB, with the exception of the half of the HBL box to the left of the diagonal line that extends from (0.8,0.55) to (1.4,0.2). We will return to this subject in § 4.

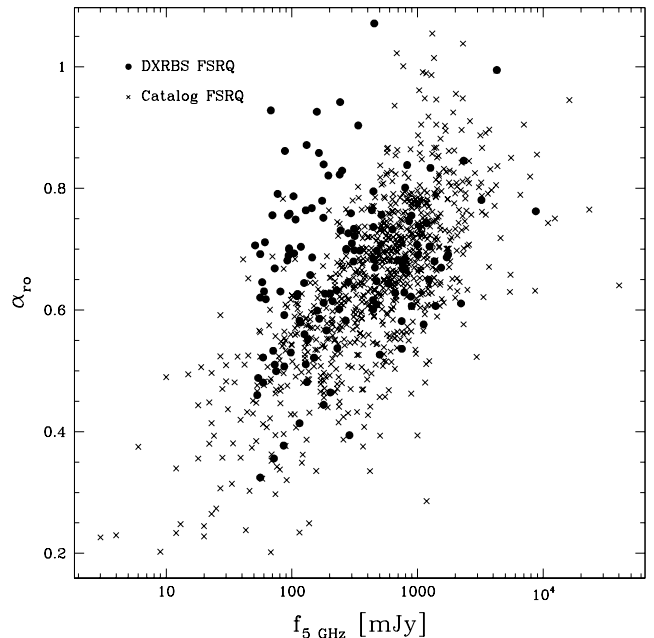


FIG. 2.— The effective radio-optical spectral index α_{ro} vs. the 5 GHz radio flux for about 900 FSRQ from the multi-frequency catalog of Padovani, Giommi, & Fiore (1997) (crosses) and the DXRBS FSRQ discussed in this paper (filled points).

Another way of looking at selection effects is to consider Fig. 2, which plots α_{ro} vs. the 5 GHz radio flux for about 900 FSRQ from the comprehensive multi-frequency catalog of Padovani, Giommi, & Fiore (1997). The observed trend between radio flux and optical-radio spectral index, with stronger radio sources having steeper α_{ro} values, is likely due to two separate effects: 1. the relatively bright optical flux limits of the various samples which were included in the catalog, responsible for the lack of sources in the upper left part of the diagram. Indeed DXRBS FSRQ, which reach $V \gtrsim 23$, start to fill this region (filled points in Fig. 2); 2. the fact that well-known, “classical” FSRQ, all relatively strong radio sources (3C 273 and 3C 279, for example, have 5 GHz radio fluxes ~ 16 and 40 Jy respectively) do have steep α_{ro} , which accounts for the lack of sources in the lower right part of the diagram. Since HF-FSRQ need to have $\alpha_{\text{ro}} \lesssim 0.5$ (see Fig. 1) they will start to be revealed only at fainter ($\lesssim 200 - 300$ mJy) radio fluxes, and it is only by conducting relatively faint radio surveys with X-ray information, like ours, that these sources can be identified in reasonable numbers.

There could be two possible reasons for the observations pointed out in the previous two paragraphs. Either some selection effect is at work, perhaps induced by a correlation

⁵ X-ray data are available for $\sim 65\%$ of 1 Jy FSRQ. The sources without X-ray data have $\alpha_{\text{ro}} \geq 0.63$ and therefore are all outside of the “HBL box”.

between the fraction of HFSRQ and flux, with HFSRQ being intrinsically more numerous at fainter fluxes/powers, or these sources are intrinsically rare and their detection in sizeable numbers requires large samples. We will address this issue in future DXRBS papers. Note that similar questions are perfectly appropriate as well for BL Lacs and these are the subject of some debate (see, for example, Fossati 2001, Giommi et al. 2002c).

4. SEDS AND THE NATURE OF BLAZAR EMISSION

In the previous section we have shown that recent, relatively deep, blazar samples with both radio and X-ray information have detected the hitherto unknown class of FSRQ with effective spectral indices typical of HBL. Based on our knowledge of BL Lacs, we expect these sources to have a synchrotron peak frequency ν_{peak} in the UV/X-ray band. Similarly, we would expect that the “intermediate” BL Lacs in our sample should have synchrotron peak frequencies intermediate between those seen for HBL and LBL, as demonstrated for S5 0716+714 by Giommi et al. (1999). We then need to study the SEDs of our sources.

4.1. α_{rx} Distributions

The HBL/LBL division is generally done in terms of the X-ray-to-radio flux ratio or effective radio–X-ray spectral index α_{rx} (Padovani & Giommi 1995b). While this parameter is broadly related to ν_{peak} (Padovani & Giommi 1996; Fossati et al. 1998; but see § 6.2), it is much easier to derive. Fig. 1 shows that the DXRBS FSRQ and BL Lacs seem to cluster at the edge of the HBL region, while the RGB FSRQ and BL Lacs are moving in progressively. This is due at least partly to the different flux limits of the two surveys, which sample different regions of parameter space. It does appear, however, that while the RGB BL Lacs populate a much larger area of the HBL region than DXRBS BL Lacs, this is not the case for FSRQ. Inclusion of the unclassified RGB sources with optical information does not alter this conclusion (see also below). Optically fainter sources will have relatively flat α_{ox} but most importantly relatively steep α_{ro} and so will be out of the HBL box.

Fig. 3 shows the fractional α_{rx} distribution of all DXRBS and RGB blazars. It is important to note that due to the serendipitous nature of DXRBS (and other, previous serendipitous surveys, including the EMSS), the area in which faint X-ray sources could be detected is smaller than that for brighter X-ray sources. Thus, in order to compare directly distributions of parameters related to X-ray flux, we need to “correct” by using the appropriate sky coverage – a necessary step which is seldom done – otherwise faint sources would be under-represented. We have already done this for the redshift distribution in Landt et al. (2001) and we refer the reader to that paper for further details. α_{rx} is obviously related to X-ray flux so we have de-convolved its distribution, shown in Fig. 3. We follow this practice for all comparisons involving DXRBS and any other serendipitous survey.

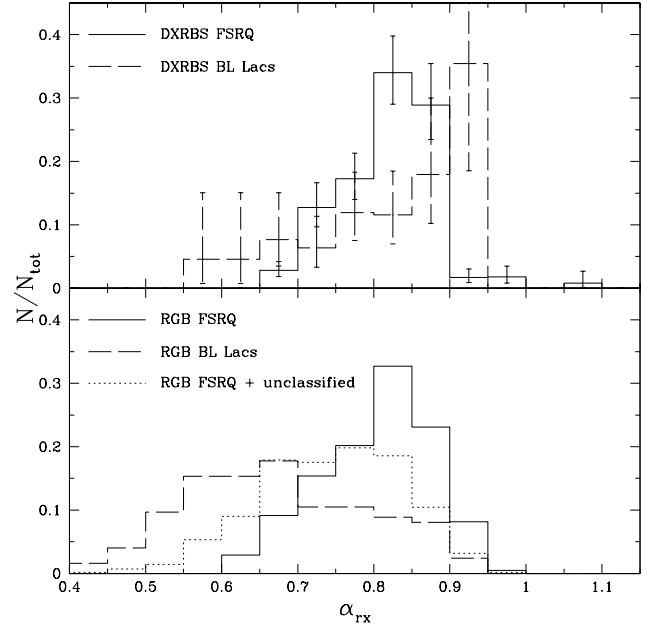


FIG. 3.— The fractional distribution of the X-ray-radio spectral index α_{rx} for FSRQ (solid lines) and BL Lacs (dashed lines) for the DXRBS (top) and RGB (bottom) samples. The dotted line represents the α_{rx} distribution of RGB FSRQ and unclassified radio-loud sources with $\alpha_{\text{r}} \leq 0.5$. The DXRBS distributions have been de-convolved with the appropriate sky coverage. Error bars represent the 1σ range based on Poisson statistics. See text for details.

A few points can be inferred from Fig. 3. The $\langle\alpha_{\text{rx}}\rangle$ values for DXRBS FSRQ and BL Lacs are similar, ~ 0.83 , but the variances are different at the 99.96% level (Student’s t-test). Moreover, the two distributions are different at the 99.4% level according to a Kolmogorov-Smirnov (KS) test. The BL Lac α_{rx} distribution, in fact, is broader than that of FSRQ, with a peak at $\alpha_{\text{rx}} \sim 0.9$ and a tail reaching relatively low values (~ 0.55). The skewness of the BL Lac distribution is negative and equal to ~ 3.4 times its standard deviation, unlike the FSRQ distribution for which the skewness is consistent with being zero (Press et al. 1986). The different nature of the BL Lac and FSRQ α_{rx} distributions is confirmed by the use of the KMM algorithm, developed by Ashman, Bird, & Zepf (1994), which computes for a given distribution the confidence level at which a single Gaussian fit can be rejected in favor of a double Gaussian fit. While for the DXRBS FSRQ we find that a single Gaussian provides a good fit to the α_{rx} distribution, this possibility is rejected at the 99.9% level for the BL Lacs. The ~ 10 still unidentified sources with $\alpha_{\text{r}} \leq 0.5$ are X-ray faint and therefore have relatively large $\langle\alpha_{\text{rx}}\rangle \sim 0.9$. Based on our identification statistics, we expect most of them to be FSRQ, thereby somewhat reducing the difference in the α_{rx} distributions at large values in Fig. 3. The fraction of sources with $L_{\text{x}}/L_{\text{r}} > 10^{-6}$, i.e., $\alpha_{\text{rx}} \lesssim 0.78$ is $\sim 28\%$ and $\sim 25\%$ for the BL Lacs and FSRQ respectively. More interesting is the fraction of sources which fall into the region typical of HBL, the “HBL box”. This is $\sim 15\%$ and $\sim 9\%$ for the BL Lacs and FSRQ respectively. For RGB the α_{rx} distributions for FSRQ and BL Lacs are also significantly different ($P > 99.99\%$), but in this case the mean values are

also different, with $\langle\alpha_{\text{rx}}\rangle \sim 0.80$ and ~ 0.68 respectively. The fraction of sources with $L_x/L_r > 10^{-6}$ is $\sim 76\%$ and $\sim 35\%$ for the BL Lacs and FSRQ respectively. The fraction of sources falling into the ‘‘HBL box’’ is $\sim 60\%$ and $\sim 27\%$ for the BL Lacs and FSRQ respectively. While RGB BL Lacs reach more extreme (i.e., much flatter) α_{rx} values than DXRBS ones, that is not the case for FSRQ.

Could this difference between RGB FSRQ and BL Lacs be explained as a selection effect? A large fraction ($\sim 60\%$) of the most X-ray loud RGB BL Lacs ($\alpha_{\text{rx}} < 0.7$) were already known because of dedicated surveys (EMSS, Slew, HEAO-1). Given the fact that the identification fraction of the flat-spectrum sources in RGB is quite low ($\sim 49\%$) and that the identified sources in RGB have mostly $O \leq 18.5$, it could be that the most extreme RGB FSRQ are still unclassified. We have then included with the RGB FSRQ the ~ 360 unclassified radio-loud sources with $\alpha_r \leq 0.5$ (assuming $z = 1$ for the K-correction). Note that this is an extreme assumption as a substantial fraction of these could be BL Lacs (their current fraction in the $\alpha_r \leq 0.5$ sample is $\sim 30\%$). Although the α_{rx} distribution now shifts to lower values, with $\langle\alpha_{\text{rx}}\rangle \sim 0.74$, it is still significantly different ($P > 99.99\%$) from that of the RGB BL Lacs. The fraction of sources with $L_x/L_r > 10^{-6}$ rises from $\sim 35\%$ to $\sim 62\%$, while that which falls into the ‘‘HBL box’’ (amongst the sources with optical information; $\sim 40\%$ of the unclassified sources are empty fields) rises from $\sim 27\%$ to $\sim 38\%$. As discussed above, this fraction should probably be considered an upper limit.

We point out that the DXRBS and RGB α_{rx} distributions for both FSRQ and BL Lacs peak at $\sim 0.7 - 0.8$, that is around the HBL/LBL dividing line. The previously suggested dichotomy in the BL Lac class then, with most sources at the two ends of the distribution, was simply due to the selection effects induced by combining widely disconnected samples selected in different bands.

We can check what happens at even larger X-ray-to-radio flux ratios by using two other samples: the EMSS and the Sedentary survey. The EMSS (e.g., Maccacaro et al. 1994) is an X-ray selected sample of sources discovered in 1,435 *Einstein* Imaging Proportional Counter (IPC) fields. It reaches $\sim 5 \times 10^{-14}$ erg cm $^{-2}$ s $^{-1}$ in the 0.3 – 3.5 keV band but the area covered is a strong function of X-ray flux (Gioia et al. 1990). The sample is largely identified (completely so down to $\sim 2 \times 10^{-13}$ erg cm $^{-2}$ s $^{-1}$) and comprehensive, dedicated radio observations provide detections down to ~ 1 mJy levels so that quite high values of X-ray-to-radio flux ratios can be reached.

Two papers have constructed samples of FSRQ within the EMSS. Wolter & Celotti (2001) constructed a sample of EMSS radio-loud quasars by using a cut $\alpha_{\text{ro}} > 0.35$. We have used the values for the thirteen FSRQ ($\alpha_r \leq 0.5$) given in their paper. Perlman et al. (2001) did a similar search which yielded those objects plus two more with $0.2 < \alpha_{\text{ro}} < 0.35$ (for consistency with the commonly used definition of radio-loud sources; these two sources happen to have the two lowest α_{rx} values). Using these objects, we have constructed the α_{rx} distribution of these EMSS FSRQ, again taking into account the effect of the sky coverage. We have also done the same for the EMSS BL Lac sample, using the revised list and data of Rector et al. (2000). The results are as follows: the α_{rx} distribu-

tions for FSRQ and BL Lacs are still significantly different ($P > 99.99\%$), with mean values $\langle\alpha_{\text{rx}}\rangle \sim 0.71$ and ~ 0.60 respectively. The minimum value reached by EMSS FSRQ is $\alpha_{\text{rx}} \sim 0.63$, while that of EMSS BL Lacs is ~ 0.49 . The fraction of sources with $L_x/L_r > 10^{-6}$, once the effect of the sky coverage is taken into account, is 100% and $\sim 78\%$ for the BL Lacs and FSRQ respectively. The fraction of sources which fall into the ‘‘HBL box’’ is the same, namely 100% and $\sim 79\%$ for the BL Lacs and FSRQ respectively. So, although the α_{rx} gap between the two classes gets narrower, the fact remains that FSRQ do not reach the same values as BL Lacs.

An even more extreme sample is the Sedentary survey (Giommi, Menna, & Padovani 1999), an X-ray/radio selected sample based on the RASS Bright Source Catalog (RASSBSC) and the NVSS, which has a cut at $\alpha_{\text{rx}} \lesssim 0.56$. The current sample is $\sim 90\%$ identified so our conclusions should be relatively stable. The number of radio-loud broad-lined sources in the sample is currently around 20 (or $\sim 12\%$), but most of these sources are very close to the radio-loud/radio-quiet dividing line, both in terms of their α_{ro} values and their radio powers. Some of these sources could therefore have their X-ray emission dominated by thermal processes and would not be the counterparts of HBL. We will discuss the presence of HFSRQ in the Sedentary survey in a future paper (Giommi et al., in preparation). Table 1 summarizes the results of these comparisons, in terms of mean α_{rx} values and fractions of HBL and HFSRQ in the DXRBS, RGB, and EMSS samples.

Our results reaffirm the fact that the percentage of HBL/HFSRQ in a sample is heavily dependent on the survey flux limits or, alternatively, its position on the X-ray–radio flux plane (see Figs. 1 and 2 of Padovani (2002)). Tab. 1 shows very explicitly how these percentages change by moving from DXRBS, a survey whose limits are in the ‘‘L’’ zone, to RGB and EMSS, whose limits move progressively deeper into the ‘‘H’’ zone.

4.2. Synchrotron Peak Frequency

To study in more detail the synchrotron peak frequencies of our sources we have used the multi-frequency information at our disposal to extract non-simultaneous SEDs for our blazars. We restrict ourselves to the DXRBS sample as the determination of ν_{peak} requires a lot more effort than α_{rx} and we did not think it was worth deriving for RGB given its large incompleteness.

We determined ν_{peak} for all 165 DXRBS blazars by applying an homogeneous synchrotron – inverse self-Compton (SSC) model in the $\log \nu - \log \nu f_\nu$ plane to the following data:

1. radio fluxes at two different frequencies (non-simultaneous 1.4 and 5 GHz data for objects with $\delta > -40^\circ$; simultaneous 5 and 8.6 GHz data for objects with $\delta < -40^\circ$; see Landt et al. 2001);
2. optical flux, in the V band, derived from Palomar Observatory Sky Survey (POSS I) O and/or E magnitudes as described in Giommi, Menna, & Padovani (1999); fluxes were corrected for Galactic absorption and for the presence of emission lines

TABLE 1
 α_{rx} STATISTICS.

Sample	FSRQ	$\langle \alpha_{\text{rx}} \rangle$		% $\alpha_{\text{rx}} \leq 0.78$			% in HBL box	
		N	BL Lacs	N	FSRQ	BL Lacs	FSRQ	BL Lacs
DXRBS	0.827 ± 0.005	134	0.84 ± 0.02	31	25%	28%	9%	15%
RGB	$0.803 \pm 0.005 (\gtrsim 0.74)$	233	0.68 ± 0.01	129	35% ($\lesssim 62\%$)	76%	27% ($\lesssim 38\%$)	60%
EMSS	0.71 ± 0.02	15	0.60 ± 0.01	41	78%	100%	79%	100%

(for FSRQ) according to the prescription of Natali et al. (1998);

- unabsorbed ROSAT X-ray flux at 1 keV, derived from the broad-band flux and the X-ray spectral index α_x ;
- Two Micron All Sky Survey (2MASS) data (if available; Cutri et al. 2000);
- any other NASA/IPAC Extragalactic Database (NED) data.

We note that here and in the following we deal with the rest-frame peak frequency, equal to $\nu_{\text{peak}}(\text{obs}) \times (1+z)$. A redshift of 0.4 was assumed for the BL Lacs without one.

While we have optical spectra for all objects identified in Perlman et al. (1998) and Landt et al. (2001), we did not use those spectra to estimate peak frequencies for two reasons. First, the DXRBS includes also a significant number of previously known sources (about 40% for the sample used in this paper), for which optical spectra are not necessarily available in digital format. We felt it would be inconsistent to use optical spectra for some objects but not for others. Second, for many objects the spectra were taken with a slit that was not at parallactic angle due to the instrumental setups used (see Perlman et al. 1998 and Landt et al. 2001). This results in a flux loss due to atmospheric differential refraction which is more pronounced in the blue part of the spectrum and would therefore significantly affect the optical/UV slope.

The SSC model was been adapted from Tavecchio, Maraschi & Ghisellini (1998) and assumes that radiation is produced by a population of relativistic electrons emitting synchrotron radiation in a single zone of a jet that is moving at relativistic speed and at a small angle to the line of sight. These photons are subsequently scattered by the same electrons to higher energies via the inverse Compton process (note that we ignore Comptonization of external photons, which only affects the SED at γ -ray energies; e.g., Ghisellini et al. 1998). The physical parameters that define the model are the jet radius, the Doppler factor δ , the magnetic field B , and four spectral parameters of the electron population, assumed to follow a power-law distribution which breaks sharply above a given energy: the normalization, the two spectral slopes, and the break energy. The Klein-Nishina cross section is used in the computation of the Compton scattering.

Our aim is to derive a best estimate of ν_{peak} . Given that the SED of most of our sources is not well sampled we cannot fully constrain the model parameters. However, the available range was limited by physical considerations, namely: $\delta \sim 10 - 20$, $B \sim 0.1 - 5$ G, jet radius $\approx 10^{-3}$

parsec, and a low-energy slope of the electron distribution which produces a relatively flat (< 0.7) spectral slope in the radio band, consistent with the sample definition. We have also been guided by the work done by some of us using the same model to derive ν_{peak} for a large sample of bright blazars observed by *BeppoSAX* (Giommi et al. 2002a) and from the NVSS-RASS 1 Jy survey (Giommi et al. 2002b). Both samples, in fact, include many “classical” blazars with well sampled SEDs for which the model parameters were well constrained. In any case, our experience shows that ν_{peak} , a combination of B , δ , and electron break energy, is relatively well constrained even for relatively large variations of these parameters, which affect much more the high-energy/inverse Compton part of the SED (e.g., Massaro et al. 2002).

FSRQ can have a disk (thermal) component in the optical/UV band but this, on average, makes up only $\sim 15\%$ of the continuum emission in DXRBS FSRQ (D’Elia, Padovani, & Landt 2003), and therefore should not strongly affect our derivation of ν_{peak} , at least in a statistical sense, although there are individual exceptions. This is also consistent with the relatively steep optical/UV slopes of these objects ($\alpha \sim 1.2$; Landt et al., in preparation). We think it is also unlikely that the thermal component can make a substantial contribution in the X-ray band, as our FSRQ have typical redshifts ~ 1.5 , which implies that the ROSAT band corresponds to 0.25 – 6 keV rest-frame. By comparison, there is very little evidence for thermal optical/UV emission due to an accretion disk in BL Lacs, although Corbett et al. (2000) have suggested that accretion disk illumination is responsible for the variations in H α luminosity in BL Lacertae itself. In any case, however, the line luminosity of DXRBS BL Lacs is much lower than that of FSRQ (Landt et al., in preparation), so that any contribution to the total optical/UV flux is negligible for our purposes.

Previous works have derived ν_{peak} by fitting analytical functions, such as a parabola or a third-degree polynomial, to the SED of blazars (e.g., Sambruna et al. 1996; Fossati et al. 1998). Although the latter alternative would also allow us to take into account the spectral upturn which is present when the X-ray flux is dominated by inverse Compton emission, we chose instead to derive ν_{peak} using a physical model (SSC) which is widely accepted as being responsible for the broad-band emission of blazars. We believe that our approach, although more complex and time consuming, is more robust especially when dealing with sparsely sampled SEDs, as we are guided by physics rather than just analytical fitting. We also note that our multifrequency data are not simultaneous and therefore our fits are also affected by variability.

As examples, in Figs. 4 and 5 we show some representa-

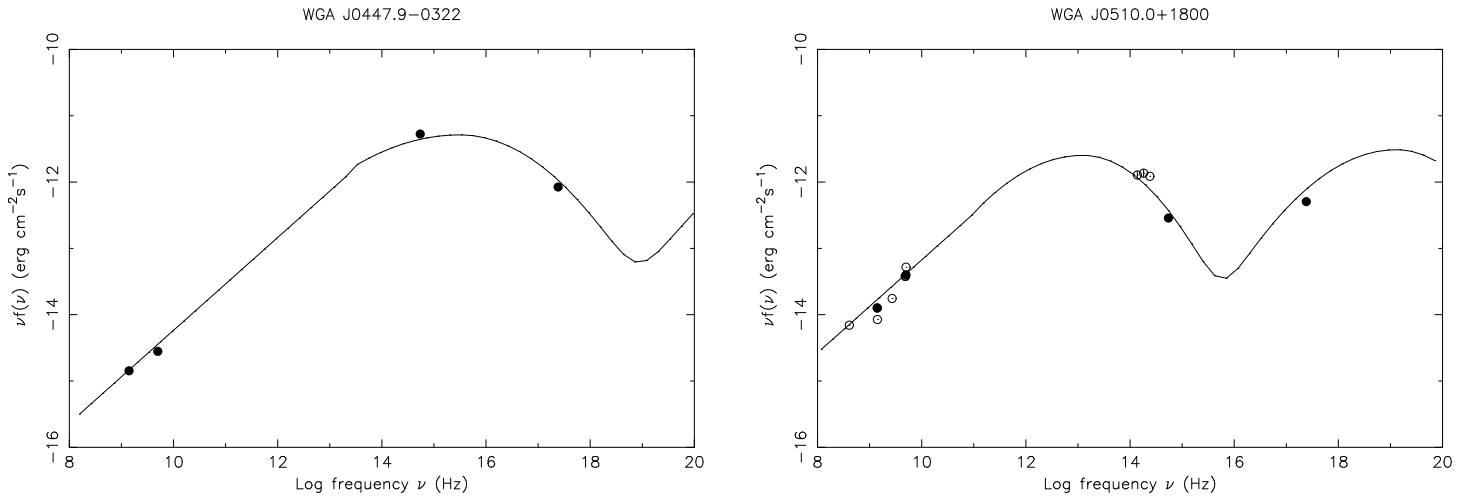


FIG. 4.— Representative synchrotron self-Compton fits to the spectral energy distributions of DXRBS FSRQ. Filled points denote DXRBS data, empty points denote data from NED and 2MASS. The synchrotron peak frequency for the two sources are $\nu_{\text{peak}} = 5.5 \times 10^{15}$ Hz (WGA J0447.9-0322, $z = 0.774$, left) and $\nu_{\text{peak}} = 1.7 \times 10^{13}$ Hz (WGA J0510.0+1800, $z = 0.416$, right). See text for details.

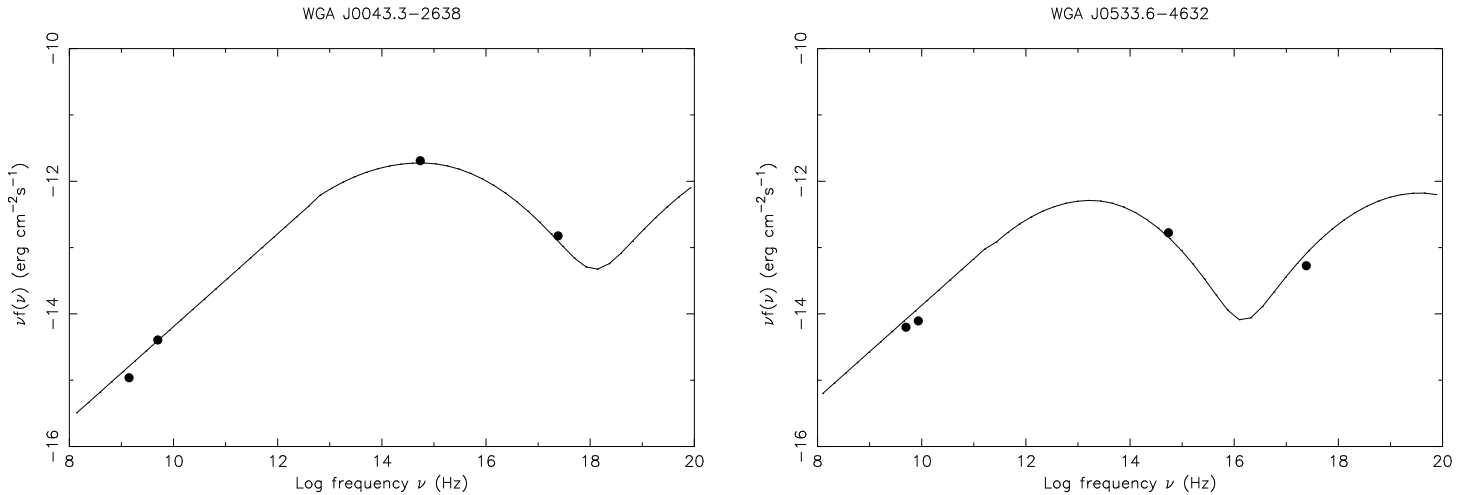


FIG. 5.— Representative synchrotron self-Compton fits to the spectral energy distributions of DXRBS BL Lacs. Filled points denote DXRBS data. The synchrotron peak frequency for the two sources are $\nu_{\text{peak}} = 1.1 \times 10^{15}$ Hz (WGA J0043.3-2638, $z = 1.002$, left) and $\nu_{\text{peak}} = 2.3 \times 10^{13}$ Hz (WGA J0533.6-4632, $z = 0.332$, right). See text for details.

tive fits to the SEDs of DXRBS FSRQ and BL Lacs, spanning a wide range of ν_{peak} . We stress again that the sampling of the SEDs is scanty, being based in many cases only on a few, non-contemporaneous data points, so that the precise value of ν_{peak} for a given source can be somewhat uncertain. However, we do believe that its *statistical* use is warranted. This is confirmed by plotting the optical/UV slopes, which are measured for 68 ($\sim 51\%$) of our FSRQ and did not enter in our derivation of the synchrotron peak frequency, vs. ν_{peak} . A very strong anti-correlation ($P = 99.96\%$) is observed between the two quantities, as expected if our ν_{peak} estimates were indeed reliable. For relatively small ν_{peak} values, in fact, one expects the opti-

cal band to sample the steep tail of the synchrotron component, while when the synchrotron peak moves to progressively larger energies the optical slope becomes flatter as the optical band samples the lower frequency, flatter parts of the synchrotron emission.

Figure 6, which shows the ν_{peak} distribution of all our sources, illustrates the fact that indeed, the SEDs of some DXRBS FSRQ peak in the UV/X-ray band. As in the case of α_{rx} , the ν_{peak} distributions are also corrected for the effect of the sky coverage. The FSRQ distribution ranges between 10^{12} and 10^{16} Hz, with $\langle \nu_{\text{peak}} \rangle = 10^{13.70 \pm 0.06}$ Hz, while the BL Lac distribution ranges between 6×10^{12} and 8×10^{16} Hz, with $\langle \nu_{\text{peak}} \rangle = 10^{14.1 \pm 0.1}$ Hz. On aver-

age, then, BL Lacs have a synchrotron peak frequency a factor ~ 2.5 larger than that of FSRQ. The two distributions are also different at the 99.97% level according to a KS test. As was the case for α_{rx} , the BL Lac distribution is broader than the FSRQ one, with a tail reaching higher values. For example, while $\sim 64\%$ and $\sim 8\%$ of BL Lacs have $\nu_{\text{peak}} > 10^{14}$ and 10^{15} Hz, these fractions go down to $\sim 31\%$ and $\sim 4\%$ for FSRQ.

We cannot think of any reason why our method should result in lower ν_{peak} for FSRQ. Quite the opposite: both the thermal component (which is small, as discussed above) and the emission lines contamination of the optical flux (for which we correct anyway) would move the peak to *higher* values (at least with relatively low ν_{peak}). We therefore regard this difference as real.

It is likely that this difference in ν_{peak} , actually, is even larger than shown here. Due to its serendipitous nature, DXRBS is subject to incompleteness at high fluxes, since bright targets are excluded by definition not to bias the sample. We can quantify this in the following way. Approximately 50 BL Lacs with radio flux above our threshold, mostly from the 1 Jy, Slew, and EMSS samples, and off the Galactic plane have been observed by ROSAT as targets. This corresponds to a surface density $\approx 2 \times 10^{-3} \text{ deg}^{-2}$, i.e. roughly 3 – 4 sources which could not be included in our survey. This effect is more severe at high ν_{peak} values where only a few objects have been detected (see Fig. 6) and the loss of even a small number of sources could make a major difference. Note in fact that many of these BL Lacs are HBL. As regards FSRQ, although the numbers are somewhat larger, the effect at high ν_{peak} values is zero because none of the previously known (and therefore likely ROSAT targets) FSRQ had high ν_{peak} .

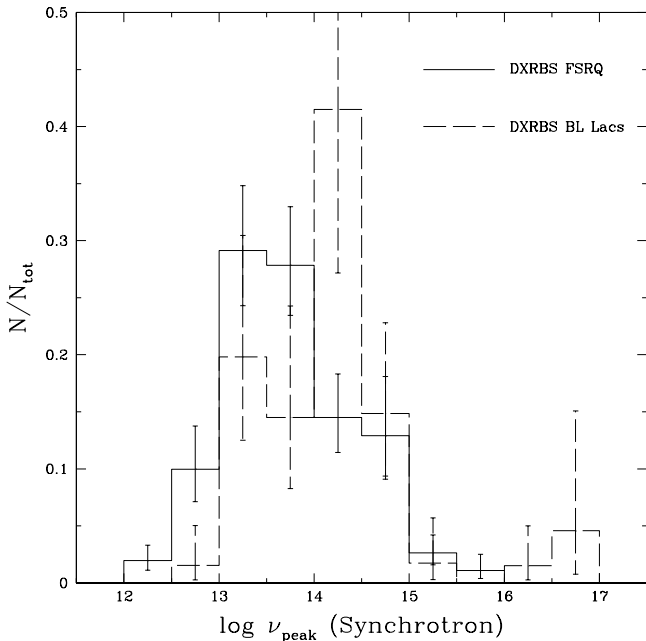


FIG. 6.— The distribution of the synchrotron peak frequency for FSRQ (solid line) and BL Lacs (dashed line) for the DXRBS sample. The distributions have been de-convolved with the appropriate sky coverage. Error bars represent the 1σ range based on Poisson statistics. See text for details.

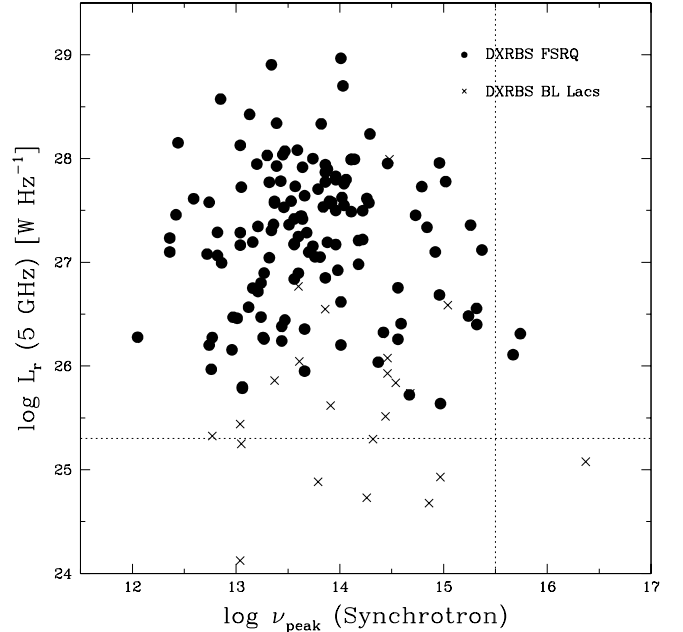


FIG. 7.— Radio power at 5 GHz vs. the synchrotron peak frequency for FSRQ (filled points) and BL Lacs (crosses) for the DXRBS sample. The dotted lines denote the two quadrants (top-left and bottom-right) occupied by the sources studied by Fossati et al. (1998). See text for details.

While already in DXRBS then there is evidence that FSRQ do not appear to reach the more extreme α_{rx} and ν_{peak} values of BL Lacs, this tendency is confirmed by studying the RGB and EMSS samples, which sample the blazar population deeper into the region of lower α_{rx} . The fact that the Sedentary survey, which samples the extreme HBL zone, has found very few, if any, FSRQ, is also suggesting that there might be an intrinsic limit to the ν_{peak} values which can be reached by strong-lined blazars.

5. THE BLAZAR SEQUENCE

Fossati et al. (1998) and Ghisellini et al. (1998) have proposed that some blazar properties can be accounted for by an inverse correlation between intrinsic power and the synchrotron peak frequency, the so-called “blazar sequence”. The peak of the emission is related to the electron energy, as $\nu_{\text{peak}} \propto B\gamma_{\text{break,e}}^2$, with $\gamma_{\text{break,e}}$ a characteristic electron energy which is determined by a competition between acceleration and cooling processes. Therefore, less powerful sources (where the energy densities are relatively small) should reach a balance between cooling and acceleration at larger ν_{peak} , while in more powerful sources there is more cooling and the balance is reached at smaller ν_{peak} .

Figure 7 plots radio power at 5 GHz versus ν_{peak} for the DXRBS sources. The dotted lines denote the two quadrants (top-left and bottom-right) occupied by the sources studied by Fossati et al. (1998), which belonged to the 1 Jy and Slew BL Lac samples and the 2 Jy FSRQ sample.

A few points can be made about this figure. First, as already shown in Fig. 6, DXRBS BL Lacs reach ν_{peak} values slightly higher than DXRBS FSRQ. (Based on the analysis shown in § 4.1 this difference is likely to become more pronounced for more X-ray extreme surveys such as

EMSS.) Second, DXRBS sources are starting to occupy regions of this plot (top-right and particularly bottom-left) which were “empty” in the original plot of Fossati et al. (1998). DXRBS reaches lower radio powers than the 1 Jy sample and therefore detects low-power LBL. In particular, out of the 21 BL Lacs with $\nu_{\text{peak}} < 10^{15.5}$ Hz and redshift information, 7 (or 33%) “invade” the low-power part ($L_r < 10^{25.3}$ W/Hz) of the plot. Third, no correlation ($P \sim 93\%$) is present between radio power and ν_{peak} for the whole sample, or for the FSRQ and BL Lac samples separately. We also note that the scatter in the plot is very large, reaching four orders of magnitude in power for $10^{13} \lesssim \nu_{\text{peak}} \lesssim 10^{15}$ Hz. Therefore, by using an homogeneous, well-defined sample which includes both FSRQ and BL Lacs over a relatively wide region of parameter space, the Fossati et al. correlation is not confirmed. Fourth, an upper envelope, however, seems to be present in the right part of the diagram. For example, all sources with $L_r > 10^{27.5}$ W Hz $^{-1}$ have $\nu_{\text{peak}} \lesssim 10^{15}$ Hz while sources with $L_r > 10^{28}$ W Hz $^{-1}$ have $\nu_{\text{peak}} \lesssim 10^{14}$ Hz.

We have checked the radio power and ν_{peak} values and distributions for DXRBS blazars in and out of the HBL box. We find that the two classes have indistinguishable radio powers but significantly different synchrotron peak frequencies, with mean values $\langle \nu_{\text{peak}} \rangle \sim 10^{15.2 \pm 0.1}$ and $\sim 10^{13.66 \pm 0.05}$ Hz respectively, again in contrast to the proposed correlation.

We note that the lack of high ν_{peak} – high radio power blazars could also be due to a selection effect, as discussed by Giommi et al. (2002c) (see also (Padovani et al. 2002)). This combination, in fact, implies a dominance of non-thermal emission over the host galaxy and emission line components, making the redshift determination very hard if not outright impossible. Objects of this kind, which would populate the upper right part of Fig. 7, would then be excluded. We note, however, that only four DXRBS BL Lacs have no redshift and $\nu_{\text{peak}} > 10^{14.5}$ Hz.

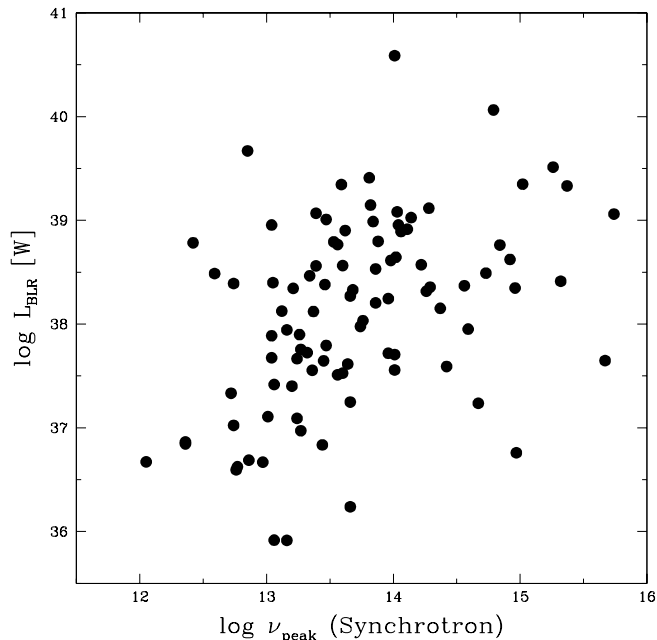


FIG. 8.— Broad Line Region luminosity vs. the synchrotron peak frequency for the DXRBS FSRQ. See text for details.

It is interesting to explore possible correlations between ν_{peak} and other powers. The correlation suggested by Fossati et al. (1998) and Ghisellini et al. (1998) was between synchrotron peak frequency and *intrinsic* power. As our sources are all flat-spectrum their radio power is strongly affected by beaming and this could influence the interpretation of Fig. 7. We have then evaluated two intrinsic powers for our FSRQ, namely the Broad Line Region (BLR) luminosity, L_{BLR} , following Celotti, Padovani, & Ghisellini (1997), and the kinetic jet power, L_{jet} , following D’Elia, Padovani, & Landt (2003).

L_{BLR} is an isotropic quantity, related to the ionizing, disk (thermal) emission via the covering factor f_{cov} , i.e., $L_{\text{disk}} = f_{\text{cov}}^{-1} L_{\text{BLR}}$, with $f_{\text{cov}} \approx 10\%$ for FSRQ (D’Elia, Padovani, & Landt 2003). Figure 8 plots L_{BLR} vs. ν_{peak} for the 94 ($\sim 70\%$) DXRBS FSRQ for which we could find the relevant BLR line fluxes. We do not include here BL Lacs because only 6 of them display the lines needed to derive L_{BLR} and even in those cases the lines are narrow. No hint of an inverse correlation between L_{BLR} , proportional to disk power, and ν_{peak} is present in the figure, the opposite is rather apparent. There is in fact a strong correlation ($P > 99.99\%$), with a large scatter, between the two quantities, with $L_{\text{BLR}} \propto \nu_{\text{peak}}^{0.51 \pm 0.11}$. It could be argued that the stronger the disk emission, the larger its contribution to the optical/UV flux, and the higher the estimated ν_{peak} . However, this is not a very likely explanation. First, as mentioned in § 4.2, D’Elia, Padovani, & Landt (2003) have shown that the disk (thermal) component in DXRBS FSRQ is only $\sim 15\%$ on average. Second, we find no correlation between L_{BLR} or ν_{peak} and the ratio of disk to total emission as defined in D’Elia, Padovani, & Landt (2003). This would be expected if larger BLR luminosities and/or larger peak frequencies were due to a stronger disk component.

It is more difficult to estimate the total kinetic jet power L_{jet} as it depends on many uncertain astrophysical parameters. We have derived it according to the prescriptions of D’Elia, Padovani, & Landt (2003), which we summarize here briefly. We have used a theoretical relationship obtained by Willott et al. (1999) to link jet power to extended radio emission at 151 MHz (using $c = 20$ in eq. 10 of D’Elia, Padovani, & Landt (2003), which agrees with another independent method), estimating the latter from the total power at 5 GHz and a correlation between core-dominance parameter and radio spectral index. We stress that, although the precise values of L_{jet} for a given source can be somewhat uncertain, we believe that its *statistical* use is warranted.

Figure 9 plots the kinetic jet power vs. ν_{peak} for our sources. No correlation is present between the two quantities. As L_{jet} is an intrinsic power, again this is in contrast with the “blazar sequence” of Fossati et al. (1998) and Ghisellini et al. (1998). Similarly to Fig. 7, however, in Fig. 9 there might be indications of an upper envelope in the right part of the diagram. For example, sources with $L_{\text{jet}} > 10^{39}$ W all have $\nu_{\text{peak}} \lesssim 10^{15}$ Hz while sources with $L_r > 10^{40}$ W have $\nu_{\text{peak}} \lesssim 10^{14}$ Hz.

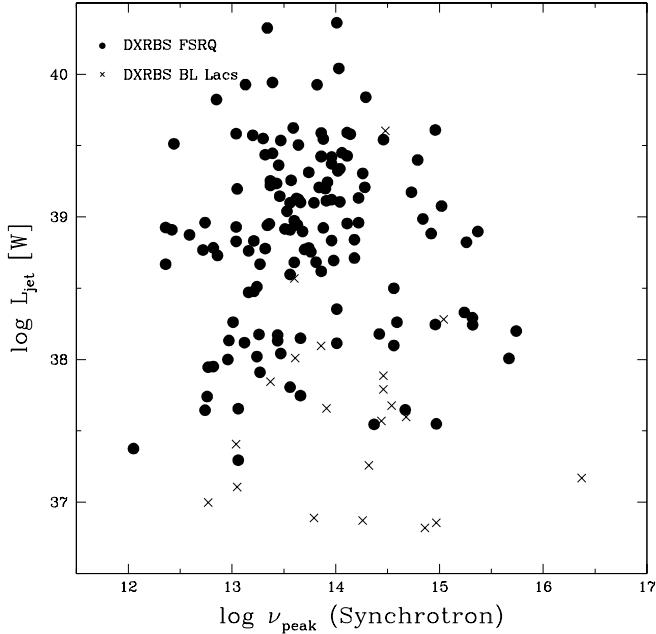


FIG. 9.— Kinetic jet power vs. the synchrotron peak frequency for the DXRBS FSRQ (filled points) and BL Lacs (crosses). See text for details.

6. FURTHER CLUES

We have shown the existence of significant numbers of FSRQ with broad-band spectra similar to those of HBL, that is with synchrotron peak frequencies higher than those of “classical” FSRQ and reaching the UV band. We now concentrate on DXRBS to further investigate the implications of our findings.

6.1. X-ray Spectral Slopes

The study of the X-ray emission of the FSRQ with synchrotron peak frequencies in the UV/X-ray band is vital. The X-ray emission of HFSRQ, in fact, should be synchrotron in nature, in contrast to that of most FSRQ, where it is dominated by inverse-Compton emission (e.g., Sambruna et al. 1996); a dichotomy similar to that exhibited by LBL and HBL. In BL Lacs, in fact, observational evidence points to a different origin for the X-ray emission of HBL and LBL (e.g., Padovani & Giommi 1996). In HBL, the X-ray continuum appears to be an extension of the synchrotron emission seen at lower energies, consistent with their steep ($\alpha_x \sim 1.5$) X-ray spectra in the ROSAT band. In LBL, the X-ray continuum is more likely due to inverse Compton emission, consistent with their harder ($\alpha_x \sim 1$) spectra. *BeppoSAX* observations of BL Lacs are confirming this picture (Wolter et al. 1998; Padovani et al. 2001). Indeed, Padovani et al. (2002) have presented evidence for at least one HFSRQ with relatively high $\nu_{\text{peak}} \sim 2 \times 10^{16}$ Hz and steep ($\alpha_x \sim 1.5$) synchrotron X-ray spectrum and two possible “intermediate” sources with $\nu_{\text{peak}} \approx 10^{15}$ Hz.

We have derived X-ray spectral indices in the 0.4 – 2.0 keV range for the DXRBS FSRQ using hardness ratios following Padovani & Giommi (1996). This method, when applied to relatively bright X-ray sources, is relatively robust and compares well with the results of a proper spec-

tral fit to the full pulse-height analyzer (PHA) spectrum. One important limitation of this method is the effect of the PSPC background, which is not subtracted off the WGACAT hardness ratios and becomes more and more important close to the sensitivity limit, especially at large off-axis angles. Fiore et al. (1998) have discussed this at length and shown that for sources with signal-to-noise ratio (SNR) > 7 background contamination is not important. However, many of the Fiore et al. (1998) sources were targets and therefore at relatively small PSPC off-sets. As DXRBS is a serendipitous survey, we have excluded all targets and therefore, on average, our sources are at larger PSPC off-sets, where the PSPC point spread function (PSF) degrades significantly, increasing the seriousness of the background contamination. We have then conservatively chosen a higher SNR cut of 10, which reduces our sample to 54 sources, 39 FSRQ and 15 BL Lacs. We stress that these effective spectral indices should still be regarded as an estimate of the “average” X-ray spectral shape and are therefore most suitable for statistical studies. Errors on these spectral indices (1σ) were derived as described in Padovani & Giommi (1996) and are typically ~ 0.2 .

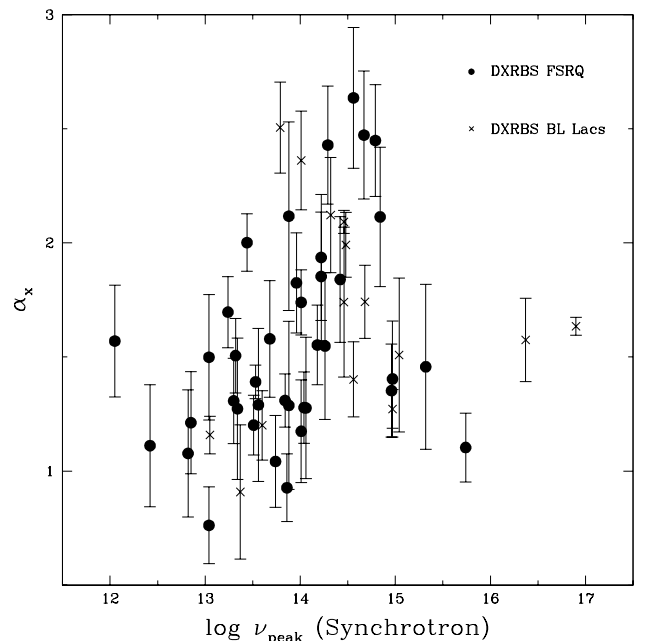


FIG. 10.— ROSAT X-ray spectral index vs. the synchrotron peak frequency for DXRBS FSRQ (filled points) and BL Lacs (crosses). Error bars represent 1σ uncertainties.

Figure 10 shows the ROSAT X-ray spectral index vs. the synchrotron peak frequency for DXRBS FSRQ (filled points) and BL Lacs (crosses). We note that α_x is relatively flat ($\sim 1 - 1.5$) and constant for $\nu_{\text{peak}} \lesssim 10^{14}$ Hz. For $10^{14} \lesssim \nu_{\text{peak}} \lesssim 10^{15}$ Hz, α_x steepens to reach values up to ~ 2.5 . Above $\nu_{\text{peak}} \sim 10^{15}$ Hz α_x flattens again to reach values $\sim 1 - 1.5$. Fig. 10 shows a trend similar

to that displayed by the BL Lacs included in Fig. 6 of Padovani & Giommi (1996), despite the fact that $\sim 70\%$ of the sources are FSRQ. We then infer that the interpretation put forward for BL Lacs applies to our FSRQ as well. Namely, at low ν_{peak} values flat inverse Compton emission dominates. For “intermediate” values the steep tail of the synchrotron component enters the ROSAT band. Finally, when ν_{peak} gets even closer to the X-ray band, the X-ray spectrum will flatten out again, because the ROSAT band is now sampling the top of the synchrotron emission.

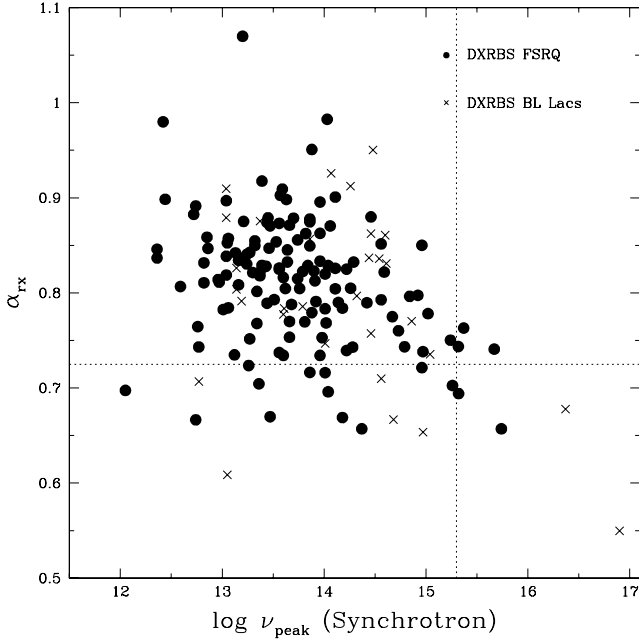


FIG. 11.— Radio-X-ray spectral index α_{rx} vs. synchrotron peak frequency ν_{peak} for FSRQ (filled points) and BL Lacs (crosses) for the DXRBS sample. The dotted lines at $\alpha_{\text{rx}} = 0.725$ and $\log \nu_{\text{peak}} = 15.3$ denote the two quadrants (top-left and bottom-right) occupied by the sources studied by Fossati et al. (1998). See text for details.

We note that *BeppoSAX* observations of four HFSRQ candidates have given mixed results: one source is clearly synchrotron dominated, another one is clearly inverse Compton dominated, while two others have a flat X-ray spectrum with evidence of steepening at low energies, similar to intermediate BL Lacs (Padovani et al. 2002). It is, however, worth noting that the synchrotron-dominated source is the one with the lowest α_{rx} and right in the middle of the HBL box, while the Compton-dominated object has the largest α_{rx} and is at the edge of the box. *BeppoSAX* spectra of “classical” (2 Jy) FSRQ, on the other hand, are all consistently flat, with $\alpha_x \sim 0.7$, perfectly explained by inverse Compton emission (Tavecchio et al. 2002; Giommi et al. 2002a). Sambruna, Chou, & Urry (2000) reported on *ASCA* observations of four FSRQ characterized by steep ROSAT spectra ($\alpha_x \sim 1.3$). The sources were all found to have flat hard X-ray spectra, with $\alpha_x \sim 0.8$. Sambruna et al. discuss their results in terms of relatively high synchrotron peaks and thermal emission extending into the X-ray band. Importantly, their sources sample a region of parameter space widely different from ours. Their effective spectral indices place

them firmly in the LBL region, unlike ours, so that they should not have been expected to show high ν_{peak} values and steep *ASCA* spectra.

As shown in § 4.2, the ν_{peak} distributions are continuous and peak at $\approx 10^{14}$ Hz for both FSRQ and BL Lacs. While on this basis there appears to be no need for dividing blazars into “H” (high-energy) and “L” (low-energy) subclasses, the picture that comes out for FSRQ is the same as that already known for BL Lacs (e.g., Padovani & Giommi (1996)), that is one of a division which can be based on physical grounds with “H” sources as those whose X-ray band is dominated by synchrotron emission and “L” sources as those in which inverse Compton dominates.

6.2. Synchrotron Peak Frequency vs. Effective Spectral Indices

It has been suggested in the literature (e.g., Padovani & Giommi 1995b, 1996; Fossati et al. 1998) that the blazar synchrotron peak frequency can be estimated from the values of the effective spectral indices. We address this point here by using for the first time a large, homogeneous and well-defined sample of blazars.

Figure 11 plots α_{rx} vs. ν_{peak} . As can be seen, the two parameters correlate quite well (the correlation is significant at the $> 99.9\%$ level for the whole sample and the FSRQ and at the 98% level for BL Lacs). However, there is considerable scatter - for any given value of α_{rx} the scatter in ν_{peak} is more than a decade. This is much more than reported in this relationship by Fossati et al. (1998), whose Figure 8 shows a correlation with typically less than a decade of scatter, particularly for $\nu_{\text{peak}} \gtrsim 10^{14}$ Hz. A careful comparison shows that the major difference between the two plots occurs at low α_{rx} . The plot in Fossati et al. shows that for $\nu_{\text{peak}} \lesssim 10^{15.3}$ Hz there are no objects with $\alpha_{\text{rx}} \lesssim 0.75$, while for $\nu_{\text{peak}} \gtrsim 10^{15.3}$ Hz the exact opposite is the case. We have drawn these regions on Figure 11 (dotted horizontal and vertical lines). With DXRBS, however, we see a different picture. As Figure 11 shows, DXRBS has effectively expanded the accessible region of parameter space by making accessible the region $0.65 \lesssim \alpha_{\text{rx}} \lesssim 0.75$ in the bottom left quadrant. The resulting increase in accessible parameter space is huge: while for objects with $10^{12} \lesssim \nu_{\text{peak}} \lesssim 10^{13}$ Hz this is only about 20%, it is more than 50% for objects with $10^{14} \lesssim \nu_{\text{peak}} \lesssim 10^{15}$ Hz. A look at Figure 11 shows that while the correlation is still highly significant, the plot looks very different at the high α_{rx} end than it does at low α_{rx} . At high α_{rx} we see a clear envelope, while it is obvious that we do not see an envelope at low α_{rx} . In other words a DXRBS blazar with $\alpha_{\text{rx}} \sim 0.7$ is just as likely to have $\nu_{\text{peak}} \sim 10^{12}$ Hz as it is to have $\nu_{\text{peak}} \sim 10^{16}$ Hz. We note that the sources with relatively low α_{rx} and ν_{peak} values are the DXRBS sources in the upper-left part of Fig. 1 which have low α_{rx} but are outside of the HBL box.

What is the reason behind this difference? In the first place the models are different: Fossati et al. (1998) used a simple third-degree polynomial fit, while the model we use is based upon a calculation of synchrotron and inverse-Compton spectra for reasonable physical parameters. More importantly, however, all the samples used by Fossati et al. - the 1 Jy, 2 Jy and Slew surveys - are classic, high flux limit surveys in the radio and X-rays re-

spectively. As shown in § 3, this type of survey has the effect of imposing what amounts to severe selection biases. This can in fact be seen in Figure 8 of Fossati et al. (1998), where both their $\nu_{\text{peak}} - \alpha_{\text{rx}}$ and $\nu_{\text{peak}} - \alpha_{\text{ro}}$ plots are seen to be discontinuous, hardly surprising considering that all but one of the objects with $\nu_{\text{peak}} > 10^{15.3}$ Hz in the Fossati et al. study is found in the Einstein Slew Survey but not the 1 Jy (only 2/34 1 Jy BL Lacs fall in the lower right hand quadrant of our Figure 11 as denoted by the two dotted lines, compared to 50/60 Slew BL Lacs), while the vast majority of the objects with $\nu_{\text{peak}} < 10^{15.3}$ Hz come from the 1 Jansky (33/34 1 Jy BL Lacs are in this range compared to 10/60 Slew BL Lacs).

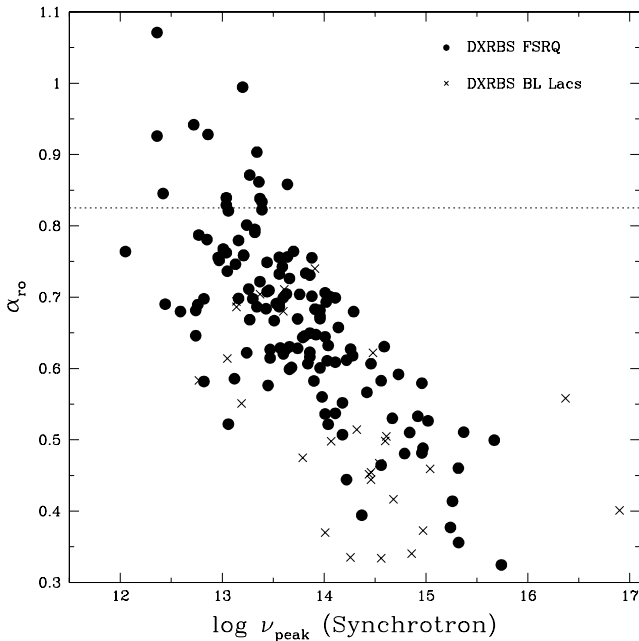


FIG. 12.— Radio-optical spectral index α_{ro} vs. synchrotron peak frequency ν_{peak} for FSRQ (filled points) and BL Lacs (crosses) for the DXRBS sample. The dotted line at $\alpha_{\text{ro}} = 0.825$ denotes the limit of the sources studied by Fossati et al. (1998). See text for details.

A tighter correlation appears to be present between α_{ro} and ν_{peak} , shown in Fig. 12. The correlation is significant at the $> 99.99\%$ level ($\sim 97\%$ for BL Lacs only), with $\alpha_{\text{ro}} \propto \nu_{\text{peak}}^{-0.12}$. This correlation is expected to break down for $\nu_{\text{peak}} \gtrsim 10^{16}$ Hz or $\alpha_{\text{ro}} \lesssim 0.4$ (Padovani & Giommi 1995b; Fossati et al. 1998) but most of our sources are outside of this range, which explains why the correlation looks almost linear. Apart from the lack of objects with $\alpha_{\text{ro}} \gtrsim 0.8$ and the paucity of objects with intermediate values of ν_{peak} Fig. 8 of Fossati et al. (1998) does not look too different from Fig. 12 in the overlapping range of ν_{peak} .

We notice that Fig. 11 shows that a definition based solely on X-ray-to-radio flux ratio or α_{rx} is not optimal, as we have found blazars with low α_{rx} and low ν_{peak} values. The position of the sources on the $\alpha_{\text{ox}}, \alpha_{\text{ro}}$ plane, which means using two (instead of one) effective spectral indices, on the other hand, appears to be more sensitive to the synchrotron peak frequency, with a difference of a factor ~ 35 in the mean ν_{peak} values for blazars in and out of the HBL

box. This is true especially for FSRQ. Fig. 1 shows, in fact, that most of the blazars with $\alpha_{\text{rx}} \leq 0.78$ but outside the HBL box are strong-lined. Tab. 1 shows also that, taking into account the sky coverage, while $\sim 54\%$ of BL Lacs with $\alpha_{\text{rx}} \leq 0.78$ are in the HBL box, this is true only for $\sim 36\%$ of the FSRQ.

6.3. Other Properties of HBL/LBL and HFSRQ/LFSRQ

We have studied the properties of blazars in and out of the HBL box not addressed in § 4, namely radio, optical, and X-ray powers and redshift. As before, distributions are “corrected” by using the sky coverage. HFSRQ have slightly smaller radio powers and slightly larger X-ray powers than LFSRQ, by factors ~ 2 , but not significantly so ($P \sim 90\%$). HFSRQ, on the other hand, have significantly ($P > 99.99\%$) larger (factor ~ 7) optical powers, due to the fact that for these sources $\langle \nu_{\text{peak}} \rangle \sim 7 \times 10^{14}$ Hz. Both classes have similar mean redshifts, ~ 1.6 and ~ 1.7 respectively, with redshift distributions which are different at the 96% level. The same comparison in the case of BL Lacs is hampered by the relatively small number statistics (18 LBL and 4 HBL with redshift). With this caveat, we find that HBL have slightly larger radio and optical powers than LBL, by factors $\sim 2 - 5$, but not significantly so ($P \sim 50\%$ and $\sim 90\%$ respectively), while they have significantly ($P \sim 98.7\%$) larger (factor ~ 35) X-ray powers. The redshift distributions for the two classes are similar with $\langle z \rangle \sim 0.4$.

If indeed all blazars that lie within the HBL “box” have radio-to-X-ray continua produced by synchrotron emission, one might expect a significant population of HFSRQ to be 100 GeV – TeV emitters. An example of such an object might be RGB J1629+4008 (Padovani et al. 2002), which has a synchrotron peak $\sim 2 \times 10^{16}$ Hz and a predicted νF_{ν} at 10^{25} Hz of nearly 10^{-10} erg $\text{cm}^{-2} \text{s}^{-1}$. A similar point was also made by Perlman (2000), albeit without the aid of BeppoSAX spectral data, who also listed five FSRQ with $\alpha_{\text{rx}} < 0.78$ and $z \leq 0.1$ derived from the RGB and *Einstein* Slew Survey. Thus the discovery of a new, X-ray loud population of FSRQ predicts the existence of a new class of 100 GeV – TeV emitting sources which could be particularly helpful for probing the diffuse infrared background at higher redshifts.

7. SUMMARY AND CONCLUSIONS

We have used the results of two recent surveys, DXRBS and RGB, to study the spectral energy distribution of about 500 blazars. Never before had this been done with a sample even remotely close to ours in terms of size, depth, and well-defined selection criteria. DXRBS, in particular, is $\sim 95\%$ complete and reaches fluxes ~ 20 times lower than previously available blazar radio surveys. We have first derived the effective spectral indices $\alpha_{\text{ox}}, \alpha_{\text{ro}}$, and α_{rx} . We have then studied the α_{rx} distributions for DXRBS, RGB, and even the EMSS samples for both FSRQ and BL Lacs. The serendipitous nature of DXRBS and the EMSS has been taken into account by “correcting” these and other distributions using the appropriate sky coverage. The synchrotron peak frequencies for DXRBS blazars have also been derived by using multi-frequency information and an homogeneous synchrotron - inverse self-Compton model. Broad line region and jet powers were also esti-

mated. One of the main aims of this work was to look for the strong-lined counterparts of high-energy peaked (HBL) BL Lacs, the HFSRQ, that is FSRQ with high-energy synchrotron peaks. We have found them. Our main results can be summarized as follows:

1. About 10% of DXRBS FSRQ have effective spectral indices typical of HBL (to be compared with 15% for BL Lacs) and can therefore be called HF-SRQ. The fractions of HFSRQ and HBL increase to $\sim 30\%$ and $\sim 60\%$ for RGB and to $\sim 80\%$ and 100% for the EMSS, respectively. Although HF-SRQ have X-ray-to-radio flux ratios larger than previously known FSRQ, in none of the samples they manage to reach values as high as those of HBL.
2. The synchrotron peak frequency distribution of DXRBS FSRQ and BL Lacs is continuous and peaks at $\approx 10^{14}$ Hz, with the former sources having an average $\nu_{\text{peak}} \sim 2.5$ times smaller than the latter. We have verified that blazars with effective spectral indices typical of HBL indeed have larger ν_{peak} values (by a factor ~ 35) than other blazars. About 60% and $> 8\%$ of DXRBS BL Lacs have $\nu_{\text{peak}} > 10^{14}$ and 10^{15} Hz respectively, to be compared with $\sim 30\%$ and $\sim 5\%$ for FSRQ.
3. These results, together with the dependence we find of the X-ray spectral index, estimated from the hardness ratios, on ν_{peak} , confirm the existence of strong-lined counterparts of high-energy peaked BL Lacs. As is the case for HBL, we would expect a significant fraction of these sources to emit at 100 GeV – TeV energies.
4. We find no anti-correlation between synchrotron peak frequency and radio, broad line region, and jet powers, contrary to the predictions of the so-called “blazar sequence” scenario, which calls for an inverse dependence of ν_{peak} on intrinsic power due to the effects of the more severe electron cooling in more powerful sources. On the other hand, available data from DXRBS and other surveys suggest that high- ν_{peak} -high-power blazars have not been found yet, and that HFSRQ do not reach the extreme synchrotron peak frequencies of BL Lacs. This indicates that after all there might be an intrinsic, physical limit to the synchrotron peak fre-

quencies and therefore electron energies which can be reached by powerful blazars.

The discovery of HFSRQ and the study of their properties have important implications for our understanding of jet formation and physics. Since $\nu_{\text{peak}} \propto \gamma_{\text{peak}}^2 \delta B$, where γ_{peak} is the Lorentz factor of the electrons emitting most of the radiation, we have shown that *powerful* jets with large magnetic fields *and* electron Lorentz factors can indeed exist – regardless of whether or not they have strong emission lines – albeit up to a point. This provides an important challenge for existing models that advocate that the spectral energy distribution of relativistic jets is strongly affected by the external radiation field. We have also shown that selection effects are very strong and that, in particular, the HBL/HFSRQ fraction is sample-dependent. Can we separate selection effects from physics? We think we can. By using DXRBS we have sampled a region of parameter space which should be largely unbiased in terms of ν_{peak} (unlike that covered by the EMSS, for example). We have found that HBL/HFSRQ make up a minority of the blazar population, $\sim 10 - 15\%$. We then believe that the available evidence suggests that nature preferentially makes jets which peak at IR/optical energies. We will address this issue in detail in a future paper.

It is also clear that, although a consistent picture comes out of our results, we need more information on these sources. We are planning dedicated X-ray observations of our newly discovered HFSRQ to further constrain their X-ray emission processes.

EP acknowledges support from NASA grants NAG5-9995 and NAG5-10109 (ADP) and NAG5-9997 (LTSA). HL acknowledges financial support from the Deutscher Akademischer Austauschdienst (DAAD) and the STScI DDRF grants D0001.82260 and D0001.82299. This research has made use of the NASA/IPAC Extragalactic Database (NED), which is operated by the Jet Propulsion Laboratory, California Institute of Technology, under contract with the National Aeronautics and Space Administration, and of data products from the Two Micron All Sky Survey, which is a joint project of the University of Massachusetts and the Infrared Processing and Analysis Center/California Institute of Technology, funded by the National Aeronautics and Space Administration and the National Science Foundation.

REFERENCES

- Ashman, K. M., Bird, C. M., & Zepf, S. E. 1994, *AJ*, 108, 2348
 Brinkmann, W., et al. 1997, *A&A*, 323, 739
 Celotti, A., Padovani, P., & Ghisellini, G. 1997, *MNRAS*, 286, 415
 Condon, J. J., Cotton, W. D., Greisen, E. W., Yin, Q. F., Perley, R. A., Taylor, G. B., & Broderick, J. J. 1998, *AJ*, 115, 169
 Corbett, E. A., Robinson, A., Axon, D., & Hough, J. H. 2000, *MNRAS*, 311, 485
 Cutri, R. M., et al. 2000, Explanatory Supplement to the 2MASS Second Incremental Data Release, available at: <http://www.ipac.caltech.edu/2mass/releases/second/doc/explsup.htm>
 D’Elia, V., Padovani, P., & Landt, H. 2003, *MNRAS*, in press (astro-ph/0211147)
 Fiore, F., Elvis, M., Giommi, P., & Padovani, P. 1998, *ApJ*, 492, 79
 Fossati, G., Maraschi, L., Celotti, A., Comastri, A., & Ghisellini, G. 1998, *MNRAS*, 299, 433
 Fossati, G. 2001, in *ASP Conf. Ser. 227, Blazar Demographics & Physics*, ed. P. Padovani, & C. M. Urry, 218
 Ghisellini, G., Celotti, A., Fossati, G., Maraschi, L., & Comastri, A. 1998, *MNRAS*, 301, 451
 Gioia, I. M., Maccacaro, T., Schild, R. E., Wolter, A., Stocke, J. T., Morris, S. L., & Henry, J. P. 1990, *ApJS*, 72, 567
 Giommi, P., & Padovani, P. 1994, *MNRAS*, 268, L51
 Giommi, P., et al. 1999a, *A&A*, 351, 59
 Giommi, P., Menna, M. T., Padovani, P. 1999b, *MNRAS*, 310, 465
 Giommi, P., Capalbi, M., Fiocchi, M., Memola, E., Perri, M., Piranomonte, S., Rebecchi, S., & Massaro, E. 2002a, in *Blazar Astrophysics with BeppoSAX and Other Observatories*, ed. P. Giommi, E. Massaro, & G. Palumbo (Frascati: ASI), 63
 Giommi, P., Perri, M., Piranomonte, S., & Padovani, P. 2002b, in *Blazar Astrophysics with BeppoSAX and Other Observatories*, ed. P. Giommi, E. Massaro, & G. Palumbo (Frascati: ASI), 123
 Giommi, P., Padovani, P., Perri, M., Landt, H., & Perlman, E. 2002c, in *Blazar Astrophysics with BeppoSAX and Other Observatories*, ed. P. Giommi, E. Massaro, & G. Palumbo (Frascati: ASI), 133

- Gregory, P. C., & Condon, J. J. 1991, *ApJS*, 75, 1011
- Gregory, P. C., Scott, W. K., Douglas, K., & Condon, J. J. 1996, *ApJS*, 103, 427
- Irwin, M., Maddox, S., & McMahon, R. G. 1994, *Spectrum*, 2, 14
- Jannuzi, B. T., Smith, P. S., & Elston, R. 1994, *ApJ*, 428, 130
- Kock, A., Meisenheimer, K., Brinkmann, W., Neumann, M., & Siebert, J. 1996, *A&A*, 307, 475
- Kollgaard, R. I., Palma, C., Laurent-Muehleisen, S. A., & Feigelson, E. D. 1996, *ApJ*, 465, 115
- Landt, H., Padovani, P., Perlman, E., Giommi, P., Bignall, H., & Tzioumis, A. 2001, *MNRAS*, 323, 757
- Landt, H., Padovani, P., & Giommi, P. 2002, *MNRAS*, 336, 945
- Laurent-Muehleisen, S. A., Kollgaard, R. I., Moellenbrock, G. A., & Feigelson, E. D. 1993, *AJ*, 106, 875
- Laurent-Muehleisen, S. A. 1996, Ph. D. Thesis, Pennsylvania State Univ.
- Laurent-Muehleisen, S. A., Kollgaard, R. I., Ryan, P. J., Feigelson, E. D., & Brinkmann, W. 1997, *A&AS*, 122, 235
- Laurent-Muehleisen, S. A., Kollgaard, R. I., Ciardullo, R., Feigelson, E. D., Brinkmann, W., & Siebert, J. 1998, *ApJS*, 118, 127
- Laurent-Muehleisen, S. A., Kollgaard, R. I., Feigelson, E. D., Brinkmann, W., & Siebert, J. 1999, *ApJ*, 525, 127
- Maccacaro, T., Wolter, A., McLean, B., Gioia, I. M., Stocke, J. T., Della Ceca, R., Burg, R., & Faccini, R. 1994, *Astrophys. Lett.*, 29, 267
- Massaro, E., et al. 2002, *A&A*, in press
- Morris, S. L., Stocke, J. T., Gioia, I. M., Schild, R. E., Wolter, A., Maccacaro, T., & Della Ceca, R. 1991, *ApJ*, 380, 49
- Nass, P., Bade, N., Kollgaard, R. I., Laurent-Muehleisen, S. A., Reiners, D., & Voges, W. 1996, *A&A*, 309, 419
- Natali, F., Giallongo, E., Cristiani, S., & La Franca, F. 1998, *AJ*, 115, 397
- Padovani, P., & Giommi, P. 1995a, *MNRAS*, 277, 1477
- Padovani, P., & Giommi, P. 1995b, *ApJ*, 444, 567
- Padovani, P., & Giommi, P. 1996, *MNRAS*, 279, 526
- Padovani, P., Giommi, P., & Fiore, F. 1997, *Mem. Soc. Astron. Italiana*, 68, 147
- Padovani, P. et al. 2001, *MNRAS*, 328, 931
- Padovani, P. 2002, in *Blazar Astrophysics with BeppoSAX and Other Observatories*, ed. P. Giommi, E. Massaro, & G. Palumbo (Frascati: ASI), 101
- Padovani, P., Costamante, L., Ghisellini, G., Giommi, P., & Perlman, E. 2002, *ApJ*, 581, 895
- Perlman, E. S., & Stocke, J. T. 1993, *ApJ*, 406, 430
- Perlman, E. S., Padovani, P., Giommi, P., Sambruna, R., Jones, L. R., Tzioumis, A., & Reynolds, J. 1998, *AJ*, 115, 1253
- Perlman, E. S. 2000, in *GeV-TeV Gamma Ray Astrophysics Workshop: Towards a Major Atmospheric Cherenkov Detector VI*, ed. B. Dingus, M. Salamon and D. Kieda (AIP: Provo), p. 53
- Perlman, E. S., et al. 2001, in *ASP Conf. Ser. 227, Blazar Demographics & Physics*, ed. P. Padovani, & C. M. Urry, 200 Press, W. H., Flannery, B. P., Teukolsky, S. A., & Vetterling, W. T. 1986, *Numerical Recipes* (Cambridge: CUP)
- Rector, T. A., Stocke, J. T., & Perlman, E. S. 1999, *ApJ*, 516, 145
- Rector, T. A., Stocke, J. T., Perlman, E. S., Morris, S. L., & Gioia, I. M. 2000, *AJ*, 120, 1626
- Reich, W., Fuerst, E., Reich, P., Kothes, R., Brinkmann, W., & Siebert, J. 2000, *A&A*, 363, 141
- Sambruna, R., Chou, L., & Urry, C. M. 2000, *ApJ*, 533, 650
- Sambruna, R. M., Maraschi, L., & Urry, C. M. 1996, *ApJ*, 463, 444
- Stocke, J. T., Morris, S. L., Gioia, I. M., Maccacaro, T., Schild, R., Wolter, A., Fleming, T. A., & Henry, J. P. 1991, *ApJS*, 76, 813
- Tavecchio, F., Maraschi, L., & Ghisellini, G. 1998, *ApJ*, 509, 608
- Tavecchio, F., et al. 2002, *ApJ*, 575, 137
- Urry, C. M., & Padovani, P. 1995, *PASP*, 107, 803
- White, N. E., Giommi, P., & Angelini, L. 1995, database at <http://wgcacat.gsfc.nasa.gov>
- Willott, C. J., Rawlings, S., Blundell, K. M., & Lacy, M. 1999, *MNRAS*, 309, 1017
- Wolter, A., et al. 1998, *A&A*, 335, 899
- Wolter, A., & Celotti, A. 2001, *A&A*, 371, 527